Study of octupole correlations in ^{90}Zr and ^{91}Zr isotopes

Ł. W. Iskra[1],* R. Mărginean[2],† S. Bottoni[3,4], N. Mărginean[2], B. Fornal[1], S. Leoni[3,4], G. Colò[3,4], L. Stan[2], R. Borcea[2], M. Boromiza[2], S. Călinescu[2], N. Cieplicka-Oryńczak[1], C. Clisu-Stan[2], C. Costache[2], F.C.L. Crespi[3,4], D. Filipescu[2], N. Florea[2], I. Gheorghe[2], A. Ionescu[2], R. Lică[2], C. Mihai[2], R.E. Mihai[2], C.R. Niţă[2], S. Pascu[2], C. Petrone[2], S. Toma[2], A. Turturică[2], and S. Ujeniuc[2]

[1]*Institute of Nuclear Physics, PAN, 31-342 Kraków, Poland*

[2]*Horia Hulubei National Institute of Physics and Nuclear Engineering—IFIN HH, Bucharest 077125, Romania*

[3]*Dipartimento di Fisica, Università degli Studi di Milano, 20133 Milano, Italy and*

[4]*INFN Sezione di Milano, 20133, Milano, Italy*

(Dated: November 4, 2024)

The $B(E3)$ transition strengths in ^{90}Zr and ^{91}Zr isotopes were determined based on the half-life measurements of the first 3^- and $(11/2)^-$ states, i.e., $T_{1/2} = 7.8(16)$ ps and 500(16) ps, respectively. The plunger method and fast-timing techniques were employed. The $B(E3)$ values of 16(3) and 20.5(7) W.u. for ^{90}Zr and ^{91}Zr were derived, pointing to a sizable octupole collectivity in both cases. The ^{90}Zr value complements the systematics of the octupole strength in even-even Zr isotopic chain, revealing a smooth trend between $A = 90$ and 96, which is in agreement with the pattern of octupole strength predicted by Quasiparticle Random Phase Approximation (QRPA) calculations. In ^{91}Zr, the Hybrid Configuration Mixing (HCM) model describes the $(11/2)^-$ low-energy strength in terms of a coupling of the unpaired neutron with the 3^- octupole excitation of the ^{90}Zr core, predicting a slight decrease of octupole strength which is in contrast with the experimental result. This suggests a more complex structure for the $(11/2)^-$ state in ^{91}Zr than predicted by the weak-coupling limit.

I. INTRODUCTION

In closed-shell nuclei, for neutrons and/or protons, low-energy excitations with angular momentum and parity $J^\pi = 3^-$ and enhanced $B(E3)$ transition rate to the ground state often appear [1, 2]. They are viewed as collective, reflection-asymmetric oscillations (phonons) of octupole type around the spherical equilibrium shape, as no indications of static octupole deformed shapes have been found so far, in semi-magic nuclei [3, 4]. Investigations of these octupole excitations along isotopic/isotonic chains of semi-magic nuclei can provide information on the microscopic nature of phonon states. In addition, in nuclei composed of one-valence particle and a magic core, the coupling between a phonon and the valence nucleon results in a multiplet of states which are also very useful probes of the phonon character [5–13].

Prominent examples for the existence of octupole-phonon excitation are the doubly magic ^{208}Pb and semi-magic ^{146}Gd (with the closed $N = 82$ neutron shell and $Z = 64$ proton sub-shell). In these systems, the 3^- level is the first excited state, with similar enhanced $B(E3)$ transition probabilities to the ground states (i.e., 34.0(5) and 37(2) W.u. [1], respectively), although of different microscopic origin. In ^{208}Pb, the 3^- level arises from a coherent superposition of many particle-hole excitations, none of them contributing to the wave function with an amplitude larger than 10% [14]. As a consequence, the $E3$ excitation energies observed in nuclei of the ^{208}Pb region do not exhibit any regular trend, although in ^{204}Pb, ^{206}Pb, and ^{208}Pb they appear rather close to the 2615-keV ^{208}Pb 3^- state.

In contrast, in the ^{146}Gd nucleus, the collective 3^- state is dominated by the proton $h_{11/2}d_{5/2}^{-1}$ particle-hole excitation across the $Z = 64$ sub-shell gap, and the two extra neutrons in ^{148}Gd, filling the $f_{7/2}$ orbital, contribute to further enhance the $B(E3)$ strength with $f_{7/2} \rightarrow i_{13/2}$ excitations within the neutron $N = 82$-126 shell [7]. Moving along the $N = 82$ isotones, a regular change of the lowest 3^- level energy and $B(E3)$ values is observed. In the $Z < 64$, $N = 82$ isotones (^{138}Ba, ^{140}Ce, ^{142}Nd, ^{144}Sm, up to ^{146}Gd), the successive filling of the $d_{5/2}$ proton sub-shell increases the $h_{11/2}d_{5/2}^{-1}$ contribution, and the respective 3^- level energies exhibit a regular decrease from 2881 keV in ^{138}Ba to 1579 keV in ^{146}Gd. At the same time, the measured $B(E3)$ rates go from 16.8(17) to 37(2) W.u., respectively [1], revealing a significant increase of collectivity. Above ^{146}Gd, in $Z > 64$ isotones, the filling of the $h_{11/2}$ proton subshell reduces the involvement of the $h_{11/2}d_{5/2}^{-1}$ excitation and the 3^- level energy increases again (no $B(E3)$ strength is measured in ^{148}Dy, ^{150}Er, and ^{152}Yb nuclei).

The $N = 88$ isotones represent another interesting region in terms of studying the intrinsic electric octupole moments. In this isotonic chain, the excitation energy of the 3^- state gradually increases from ^{144}Ba (838 keV) to ^{156}Er (1304 keV) [1]. However, the corresponding $B(E3)$ strengths do not exhibit a clear regular trend, corresponding to 52(17), 33(3), and 34(3) W.u. for ^{152}Gd, ^{150}Sm, and ^{148}Nd, respectively [1]. In particular, in ^{144}Ba and its neighbour ^{146}Ba, recent Coulomb excitation measurements of $E3$ transition matrix elements show large $B(E3)$ values of 48^{+25}_{-34} W.u. [15] and 48^{+21}_{-29} W.u. [16], indicating an enhancement of octupole collectivity.

* Corresponding author: lukasz.iskra@ifj.edu.pl
† Corresponding author: raluca@tandem.nipne.ro

It is worth mentioning that in these isotopes, the stabilization of octupole deformation at high spin, around 10-12 $\hbar$, has been proposed by R. V. Jolos and P. von Brentano [17].

Phonon excitations have also been studied along the Zr ($Z = 40$) isotopic chain, starting from ^{90}Zr with closed $N = 50$ neutron shell. In analogy with the $N = 82$ isotonic chain, discussed above, the successive filling of the $d_{5/2}$ neutron orbital leads to an increase of the 3^- collectivity, resulting in $B(E3)$ rates of 18.1(11) [18], 24(8) [1] and 42(3) W.u. [19] in ^{92}Zr, ^{94}Zr, and ^{96}Zr, respectively, the latter being among the largest in the nuclear chart. The increase of octupole correlation is also reflected by the lowering of the 3^- excitation energy from 2340 keV in ^{92}Zr, to 2058, and 1897 keV in ^{94}Zr and ^{96}Zr, isotopes, respectively [1]. The energy of the 3^- state in ^{90}Zr at 2748 keV follows this trend, however, the very large $B(E3)$ value, 28.9(15) W.u. reported in Ref. [1], is out of the expected systematics.

Theoretical calculations, based on the Monte Carlo shell-model approach, reproduce well the experimental $B(E3)$ value for ^{96}Zr, and indicate that the octupole collectivity in this nucleus arises from both protons and neutrons excitations [19]. Therefore, the decreasing number of neutrons in the $d_{5/2}$ orbital in lighter Zr isotopes may be responsible for the corresponding lowering of $B(E3)$ rates in these Zr nuclei. In this context, the surprisingly large value of $B(E3)$ strength in ^{90}Zr [1], with the closed $N = 50$ neutron shell, is puzzling.

The current work focuses on the re-examination of the $B(E3)$ rate in ^{90}Zr. In addition, for the first time, the strength of the octupole collectivity in the odd ^{91}Zr isotope is also established.

In ^{90}Zr, the first two negative-parity states in the level scheme are the 5^- and $(4)^-$ states, located at 2319 and 2739 keV excitation energy, with dominant $\pi(p_{1/2}g_{9/2})$ two quasiparticle structure, the 3^- state being only the third in sequence at 2748 keV. The high-statistics (n,n'γ) measurement of Garrett *et al.* [20] reported that the 3^- state has a 93.8(3)% $E1$ branch to the 2^+ state, a 0.5(1)% $E2$ branch to the 5^- level, and a 5.7(3)% $E3$ branch to the ground state. These values have been adopted in the current analysis. Although the relevant $E3/E1$ branching in the depopulation of the 3^- state is known with a good accuracy, the 3^- half-life was not measured. What is known on the reduced transition probability of the $E3$ branch, $B(E3)$, comes from several light charged particle inelastic scattering experiments which had been conducted since early 1960's (see appropriate references in [1] and [21]). We note that most of the inelastic proton scattering data on the $E3$ strength, reported in [1], agree with the value obtained in the current analysis. However, the largely different values $B(E3) = 28.9(15)$ W.u. and $B(E3) = 8.0^{+18}_{-13}$ W.u., which are based on (e,e') [22] and (^{17}O,^{17}O$'$) [23] inelastic scattering cross section measurements, respectively, were adopted in most recent compilations [1] and [21].

In particular, the value of $B(E3) = 28.9(15)$ W.u. for the $3^- \rightarrow 0^+$ transition (from (e,e') scattering) would correspond to a half-life of $T_{1/2} = 4.2(4)$ ps of the 3^- state, after considering the branching ratio of gamma decay from that state given in [21]. It is worth noting that a very similar result of 4.7(6) ps for the 3^- half-life was quoted by Garrett *et al.* [20], based on the (e,e') data alone [22]. In turn, the value of $B(E3) = 8.0^{+18}_{-13}$ W.u. (from (^{17}O,^{17}O$'$) scattering) would correspond to a half-life of $T_{1/2} = 15.2(28)$ ps of the 3^- state [21]. The issue became even more complex, since J.R. Beene *et al.*, [26] obtained significantly higher transition rate $B(E3)$ = 21.1 W.u. (corresponding to the 3^- half-life of 5.8(6) ps), based on the same (^{17}O,^{17}O$'$) dataset [23], but using a different angular distribution fitting procedure.

There is no doubt that this situation calls for a model-independent determination of the $B(E3)$ transition rate in ^{90}Zr to probe the octupole correlation in this isotope. In the present work, the octupole collectivity in ^{90}Zr was determined by direct measurement of the half-life of the 3^- state.

The lifetime of the yrast $(11/2)^-$ state in ^{91}Zr, located at 2170 keV, also becomes a key quantity in the context of quantifying the octupole collectivity of the ^{90}Zr core. A sub-nanosecond value would imply a large $B(E3)$, which may indicate a particle-octupole phonon coupling character for this state. On the contrary, a large value around 10 ns would correspond to a $B(E3)$ strength of $\sim$1 W.u. and would indicate that this state is simply a member of the multiplet arising from the coupling of a neutron in $d_{5/2}$ with the low-lying, negative-parity two quasiparticle states of the core. So far, only an upper limit of $\sim$2000 W.u has been established for the $B(E3)$ transition rate based on the $T_{1/2} > 5.5$ ps measurement of the $(11/2)^-$ state, using the Doppler shift attenuation method [27]. In the current study, the fast-timing technique was employed to pin down the half-life of $(11/2)^-$ level and thus the strength of possible octupole correlations.

The paper is organized as follows. In Sec. II, the two different experiments performed to assess the half-life of the 3^- and $(11/2)^-$ states in ^{90}Zr and ^{91}Zr are described, while the analyses and the experimental results are presented in Sec. III. A comparison with theory predictions based on Quasiparticle Random Phase Approximation (QRPA) calculations for ^{90}Zr and on the Hybrid Configuration Mixing (HCM) model for ^{91}Zr is presented in Sec. IV, confirming the collective octupole nature of the $(11/2)^-$ state.

II. EXPERIMENTAL PROCEDURE

To investigate the nature of octupole collectivity in ^{90}Zr and ^{91}Zr isotopes, two independent experiments were conducted at the Tandem Laboratory of the Horia Hulubei National Institute for Physics and Nuclear Engineering (IFIN-HH) in Bucharest.

To populate the 3^- state in ^{90}Zr, the ^{89}Y(^{7}Li,α2n)^{90}Zr

reaction was employed, where a ^{7}Li beam, at the sub-Coulomb barrier energy of 17 MeV, bombarded a ^{89}Y target with 1 mg/cm^2 thickness. The γ-rays of interest were recorded by the ROSPHERE array [28], equipped with 20 HPGe detectors, while the 6 solar cells of SORCERER particle array [29] was used to tag on the α-like ejectiles. The SORCERER detectors were mounted inside the scattering chamber at backward angles where the maximum distribution of α particles is observed. The γ rays were emitted from the nuclei stopped in the plunger Ta stopper (5 mg/cm^2 thickness), providing Doppler-free spectroscopy. The γ-γ coincidences were collected at 7 plunger-target distances, i.e., 14, 40, 65, 130, 260 μm, and 1 and 3 mm.

In the case of ^{91}Zr, excited states were populated by the ^{82}Se(^{13}C,4n)^{91}Zr fusion-evaporation reaction. The CASCADE code was employed to calculate the cross sections for different exit channels indicating about 400 mb for the 4n evaporation channel at 42 MeV beam energy, which represents ∼80% of the total fusion cross-section. The ^{82}Se target was 5 mg/cm^2 thick, with a 5 mg/cm^2 Au backing dimensioned to stop the ^{91}Zr products, considering their optimum energy range for production. The γ rays were detected with the ROSPHERE array assembled in a mixed configuration, with 14 HPGe and 11 LaBr$_3$(Ce) scintillator detectors.

III. EXPERIMENTAL RESULTS

The partial level scheme of the ^{90}Zr isotope, together with a γ-ray spectrum gated on the stopped component of the 2186-keV $2^+ \rightarrow 0^+$ transition, is shown in Fig. 1. The spectrum was constructed by summing the spectra taken at all 7 target-to-stopper distances. Each plunger distance was normalized to the 532-keV line in ^{94}Mo (from the 2956-keV, 8^+ isomeric state, with $T_{1/2} = 98(2)$ ns [30]) produced in the ^{7}Li + ^{89}Y fusion-evaporation reaction. In this case, coincidences with α particles in the SORCERER detectors were not required. The normalization factors were also verified by considering the 184-keV transition from the 162(7) ns 5^+ isomer, located at 1121 keV in ^{18}F [31]. The latter was produced via reactions on a small amount of ^{16}O contaminants in the ^{89}Y target. In the ^{90}Zr spectrum, the 562- and 891-keV peaks correspond to the decay of the 3^- and 4^+ states, respectively. A weak $4^+ \rightarrow 3^-$, 329-keV line (from the 2.91(28)-ps level [32]) is also observed, representing about 4% of the 3^-, 2748-keV state population. It has been estimated that this feeding could increase the half-life of the 3^- state by about 0.2 ps, and it was taken into account in the final uncertainty. No other feeding of the 3^- state is observed in our data, although numerous higher located levels that decay to the 2748-keV state are reported in the NNDC database [21]. The half-lives of the lowest ten of these states are known and do not exceed 0.28 ps. Therefore, even assuming their population at the limit of observation in our experiment (∼1%), their decay to the 3^- would not affect the measurement of the half-life of this state in any significant way. We note that in the plunger spectra only lines corresponding to the stopped components are observed, as a result of the gating on the stopped component of the $2^+ \rightarrow 0^+$ transition which collects the intensities from the decay of longer-lived states.

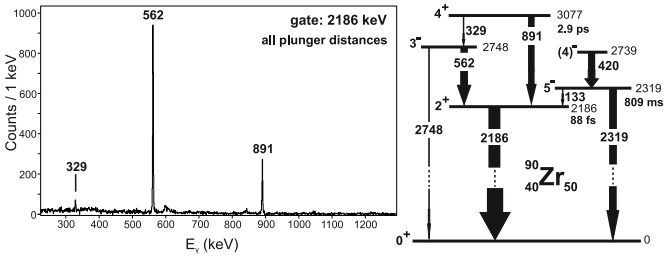

FIG. 1. Left: spectrum of ^{90}Zr in coincidence with the $2^+ \rightarrow 0^+$, 2186-keV transition, obtained by summing over all 7 plunger distances. Right: partial decay scheme of ^{90}Zr, as observed in this work, including also the $3^- \rightarrow 0^+$, $(4)^- \rightarrow 5^-$, $5^- \rightarrow 2^+$, $5^- \rightarrow 0^+$ branches from Ref. [21]. Moreover, the half-lives of the 2^+ and 5^- states have been adopted from [21], while the half-life of the 4^+ level has been taken from Ref. [32].

The thin 1 mg/cm^2 ^{89}Y target was made to maximize the reaction products that can exit the target and reach the plunger stopper. Nevertheless, a fraction of ^{90}Zr nuclei were found to be stopped inside the target, thus giving an additional contribution to the stopped peak, regardless of the stopper distance. This effect was quantified by analyzing the spectra collected at the large distances of 1 and 3 mm. They correspond to a recoil time-of-flight of more than 140 and 420 ps, respectively, for an average recoil velocity v/c ∼2%, as resulting from the kinematics. For such long distances the number of events in the stopped peak is constant, as it originates from the decay of the recoils stopped inside the target. Therefore, this contribution can be subtracted from the intensity measured at each given distance.

The spectra of ^{90}Zr, in coincidence with the $2^+ \rightarrow 0^+$ transition, measured at plunger distances of 14 and 40 μm are shown in panel (a) and (b) of Fig. 2, respectively. A fast decrease of the 891-keV transition intensity relative to the 562-keV line is observed, indicating that the half-life of 3^- state (deexcited by the 562-keV γ ray) is longer than the 2.9-ps half life of the 4^+ state (deexcited by the 891-keV transition) [32]. The decay curves of the 4^+ and 3^- excited states in ^{90}Zr, as a function of target-to-stopper distance (upper x axis), are plotted in Fig. 3 in blue and red, respectively. Knowing the half-life of the 4^+ state ($T_{1/2} = 2.91(28)$ ps, from Recoil Distance Doppler Shift (RDDS) techniques) [32], the plunger distances can be translated into decay times (lower x axis in Fig. 3). Next, by employing a fitting procedure the $T_{1/2} = 7.8(16)$ ps half-life of the 3^-, 2748-keV state was obtained.

Turning now to ^{91}Zr, this isotope was also strongly pro-

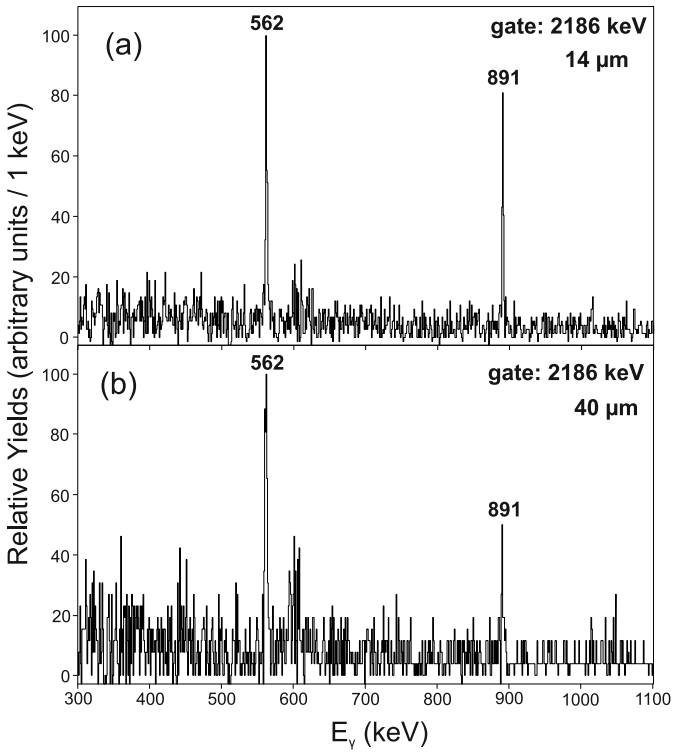

FIG. 2. Coincidence spectra in ^{90}Zr gates on $2^+ \rightarrow 0^+$ 2186-keV. Spectrum (a) and (b) represent a portion of γ coincidence events collected at target-stop distances of 14 μm and 40 μm, respectively.

duced in the ^{7}Li + ^{89}Y reaction. However, only a small decrease of the intensity of the 2170-keV, $(11/2)^- \rightarrow 5/2^+$ transition was observed over all target-to-stopper distances, leading to the $T_{1/2} > 220$ ps limit for the half-life of the $(11/2)^-$ state.

To improve the sensitivity to lifetimes in hundreds of ps range, a second experiment was performed in which the ^{91}Zr isotope was produced via the ^{13}C + ^{82}Se fusion-evaporation reaction, and the fast-timing technique was employed using the $LaBr_3$(Ce) detectors present in the array (see Sec. II). Details about the technique can be found in Ref.[33]. The $LaBr_3$ data were sorted into asymmetrical $E\gamma_2 - E\gamma_1 - \Delta T$ coincidence cubes, where $E\gamma_1$ and $E\gamma_2$ are the energy of gamma transitions in coincidence, and ΔT their difference in time. Special care was taken to keep the amplitude linearity of the $LaBr_3$(Ce) detectors and correct for constant fraction discrimination walk over a wide energy range. By applying two-dimensional energy gates on the γ rays feeding and decaying from the state of interest, time distributions were obtained for selected states in ^{90}Zr and ^{91}Zr. The $LaBr_3$ energy gating conditions were also checked by using the HPGe detectors, in order to monitor possible contaminants with higher energy resolution.

The 2^+ state in ^{90}Zr produced in ^{82}Se(^{13}C,5n)^{90}Zr fusion-evaporation reaction was used to validate the method. The time spectrum in Fig. 4(a) is constructed by

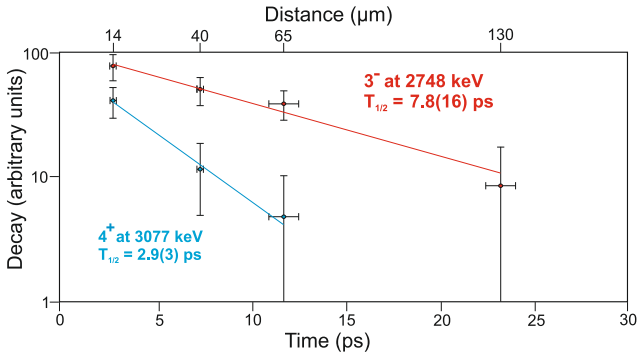

FIG. 3. Decay curves of 3^- and 4^+ states in ^{90}Zr in red and blue, respectively. The upper x-axis corresponds to target-to-stopper distances estimated on basis of the half-live of 4^+ level (i.e., $T_{1/2} = 2.9(3)$ ps), adopted from Ref. [32].

selecting the 133-keV, $5^- \rightarrow 2^+$ line as a START signal for the fast-timing analysis, while the 2186-keV transition to the ground state was the STOP. In this way, the experimental timing response of the setup was precisely determined since the half-life of the first 2^+ state of ^{90}Zr has the 88 fs value reported in [21]. The $(11/2)^-$ state in ^{91}Zr is located at similar excitation energy, only 16 keV lower. In this case, the 89 keV γ-ray feeding the $(11/2)^-$ state was selected as a START signal, while the STOP was given by the 2170-keV, $(11/2)^- \rightarrow 5/2^+$ transition. The corresponding time spectrum is shown in Fig. 4(b). By employing the fitting procedure described in Ref.[33], a half-life of 500(16) ps was obtained for the $(11/2)^-$ state in ^{91}Zr.

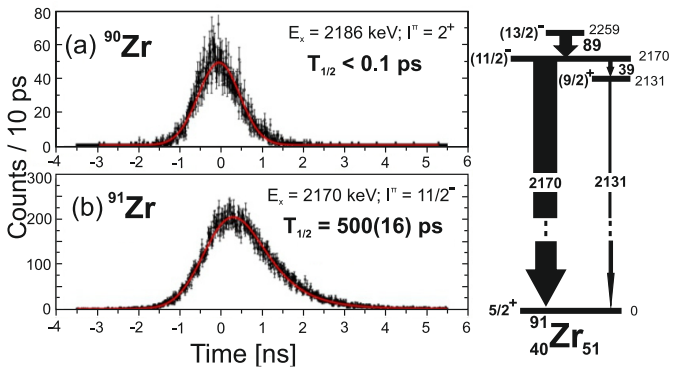

FIG. 4. Right: partial level scheme of ^{91}Zr, focusing on the decay from the $(13/2)^-$ and $(11/2)^-$ states of interest in this work. Left: Time spectra used in the fast-timing analysis of the 2^+ state in ^{90}Zr (a) and the $(11/2)^-$ state in ^{91}Zr (b), both populated in the reaction ^{13}C+^{82}Se. For the 2^+ state, start and stop energy gates were set on the 133 and 2186-keV transitions (see Fig. 1), for the $(11/2)^-$ case the 89-2170 keV energy gates were used (see right panel).

Additionally, the branching ratio from the $(11/2)^-$ state was extracted by placing a gate on the 89-keV transition and examining the intensities of the 2131- and

2170-keV lines (see Fig. 4). It is found that 93.7(2)% of the decay from the $(11/2)^-$ state goes via the 2170-keV $E3$ transition. The second decay branch, involving the 39-keV $E1$ transition with conversion coefficient of 1.71 [34], accounts for 6.3(1)% of the intensity. It is worth to note that the 3^- level in the ^{90}Zr isotope was also observed in this set of data. However, a lifetime analysis based on the fast-timing technique could not be performed, since no feeding to this state was observed.

IV. DISCUSSION

Half-lives and γ-ray branches for the 3^- and $(11/2)^-$ states in ^{90}Zr and ^{91}Zr isotopes, respectively, were used to extract the corresponding $B(E3)$ transition rates to the ground states using the formalism given in Ref. [1]. For the 3^- state in ^{90}Zr, assuming the branching ratio BR = 5.7(3)% [20], the result $B(E3) = 16(3)$ W.u. was obtained - significantly lower than the 28.9(15) W.u. value currently quoted in the compilation [1]. In turn, for the ^{91}Zr isotope the $B(E3) = 20.5(7)$ W.u. value was extracted, taking into account the 93.7(2)% branching obtained in the current measurement.

The new $B(E3)$ values were included into the systematics of octupole strength in Zr isotopes, which now displays a rather smooth increasing trend from ^{90}Zr to ^{96}Zr, accompanied by a corresponding decrease in excitation energy for the 3^- and $(11/2)^-$ states, as shown in Fig. 5(b) and Fig. 6(b). Our results are very much in line with the systematics of excitation energy and $B(E3)$ values for the 3^- states in $N = 82$ isotopes, in which the successive filling of the $d_{5/2}$ proton sub shell increases the $h_{11/2}d^{-1}_{5/2}$ contribution to the 3^- collective wave function. This is shown in Fig.5(a) and Fig.6(a).

For our theoretical analysis, in even-even nuclei we have performed Quasiparticle Random Phase Approximation (QRPA) calculations. QRPA reduces to simple RPA when there is no superfluid solution, as in ^{90}Zr. Thus, experimental results for the 3^- state in ^{90}Zr were compared with RPA calculations using different Skyrme interactions [35], which have been widely used to describe vibrational excitations. RPA calculations were performed on a Hartree-Fock basis in a box of 16 fm, including sufficient unoccupied single-particle states to guarantee the convergence of both the 3^- energy and the $B(E3)$ reduced transition probability. The results with the SLy5 [36] and SAMi-m60 [37] interactions are presented in Figs. 5, 6 and Tab. I along with experimental data. One can note that the energy of the 3^- state in ^{90}Zr is rather well reproduced by the SLy5 interaction, within ≈200 keV, while the SAMi-m60 force overestimates the experimental value by ≈ 35% due to a lower effective mass (m^*/m=0.6). In fact, the effective mass is inversely proportional to the single-particle level density, and lower effective mass results in a more stretched single-particle spectrum. The calculated $B(E3;\ 3^- \rightarrow 0^+)$ value is about 50% and 80% larger than the one measured in the present work, for the SLy5 and SAMi-m60 interactions, respectively. This can be ascribed to a high impact of octupole correlations, and to a large fragmentation of the calculated wave functions whose main components are displayed in Tab. I.

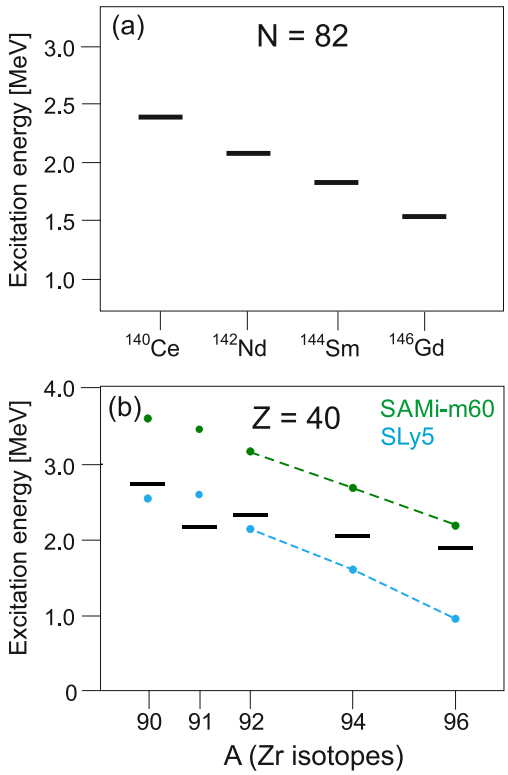

FIG. 5. Evolution of the excitation energy of the 3^- levels across the $N = 82$ isotones (a) and $Z = 40$ isotopes (b). In panel (b), the blue (green) curve gives the velues predicted by (Q)RPA calculations for the even-even Zr cores using the SLy5 (SAMi-m60) interaction. For the $(11/2)^-$ state in ^{91}Zr, predictions are given by the HCM model with both interactions (see text for details).

For completeness, similar calculations were performed in ^{92,94,96}Zr isotopes using a QRPA approach, after fixing the pairing volume term to reproduce the experimental pairing gap along $Z = 40$ (i.e., $V_0 = 740$ MeV). The results are also presented in Figs. 5, 6 and compared with experimental data. The experimental trend of the 3^- state energies is well reproduced by both interactions, with the SAMi-m60 force better predicting ^{96}Zr. On the other hand, the SLy5 interaction overestimates substantially the $B(E3;\ 3^- \rightarrow 0^+)$ values, which are better reproduced by the SAMi-m60 force, pointing to a strong sensitivity of these calculations along $Z = 40$ on the type of interaction. In particular, low-lying octupole configurations are found in these nuclei with associated large coupling matrix elements. This lies at the origin of a significant enhancement of $B(E3;\ 3^- \rightarrow 0^+)$ transition rates and is often referred to in the literature as onset of "octupole correlations".

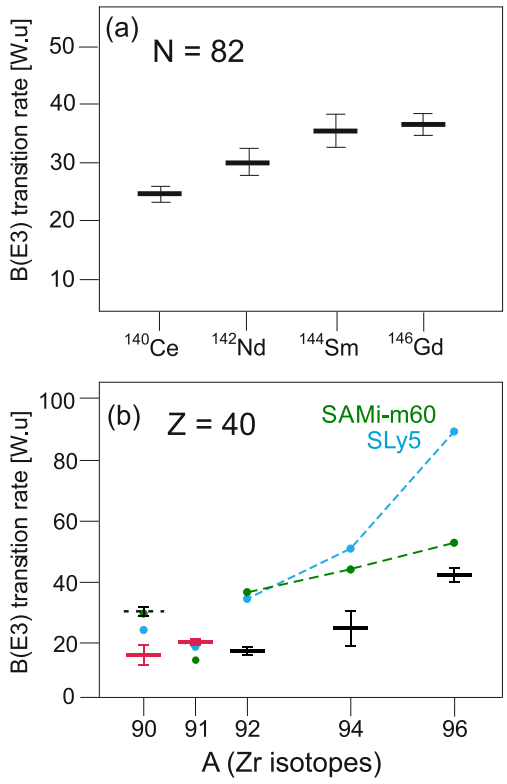

FIG. 6. Evolution of the $B(E3)$ values across the $N = 82$ isotones (a) and $Z = 40$ isotopes (b), in Weisskopf units [1]. The $B(E3)$ values in ^{90}Zr and ^{91}Zr, obtained in this work, are marked in red, while the dashed symbol gives the $B(E3)$ value for ^{90}Zr currently reported in literature [1]. In panel (b), the blue (green) curve gives the $B(E3)$ strength predicted by (Q)RPA calculations for the even-even Zr cores using the SLy5 (SAMi-m60) interaction. For the $(11/2)^-$ state in ^{91}Zr, predictions are given by the HCM model with both interactions (see text for details).

The other negative parity states, 5^- and $(4)^-$, in ^{90}Zr are also predicted by RPA calculations, with an almost pure $\pi p^{-1}_{1/2} g_{9/2}$ configuration, as shown in Tab. I. These states might correspond to the experimental 5^- state at 2.319 MeV and $(4)^-$ state at 2.739 MeV, respectively [21] For the 5^- state, an experimental $B(E5; 5^- \rightarrow 0^+)$ of 8.74(33) W.u. is reported in the literature [21], which is well reproduced by RPA calculations with both interactions.

Turning now to the odd system ^{91}Zr, the possible $(^{90}\text{Zr} \otimes \nu)$ structure of $(11/2)^-$ states in ^{91}Zr was investigated with the Hybrid Configuration Mixing (HCM) model [38], already used to calculate ^{133}Sb [39] and Ca isotopes around closed shells [40]. The HCM model is aimed at a microscopic description of odd-even nuclei with one particle/hole outside a doubly magic even-even core. The model is based on a Hamiltonian of Skyrme type, with core states, both phonons and simple 1p-1h excitations, calculated via RPA and coupled to the pure particle/hole states, with the coupling discussed in detail in Ref. [41]. In the present work, HCM model calculations were performed with the same Skyrme interactions used for the ^{90}Zr core. The model space consisted of core excitations up to 5.5 MeV, with angular momentum up to L=7, and the full $g_{7/2}sdh_{11/2}$ shell above $N = 50$ for single-neutron states. Theoretical results for $(11/2)^-$ states in ^{91}Zr are also presented in Tab. I.

Three states are found at low excitation energy with dominant $(3^- \otimes \nu d_{5/2})$, $(4^- \otimes \nu d_{5/2})$, and $(5^- \otimes \nu d_{5/2})$ character. While in the case of the SLy5 interaction, the three states have a one-to-one correspondence with the couplings mentioned above, for the SAMi-m60 force there is some amount of mixing. The overall $B(E3)$ value in this low-energy region is, in both cases, comparable with the experimental findings. However, we note that the HCM model does not reproduce the enhancement of octupole collectivity with respect to the ^{90}Zr core, as measured in this work, hinting at the possible presence of more complicated components in the wave function of the $(11/2)^-$ state, beyond the $2p - 1h$ components included in the HCM model space. We finally note that a C^2S, spectroscopic factor of 0.40 was found for the ℓ=5, $(11/2)^-$ state at 2.170 MeV in a recent ^{90}Zr(d,p) experiment [42], pointing to a reduced $h_{11/2}$ strength at low excitation energy in ^{91}Zr, in fair agreement with the HCM model. This can again be ascribed to the $(^{90}\text{Zr} \otimes \nu)$ couplings which dominate the structure of low-lying $(11/2)^-$ states in ^{91}Zr.

V. CONCLUSIONS

In summary, the current work studied the octupole excitations in the ^{90}Zr and ^{91}Zr isotopes in the context of the evolution of $B(E3)$ transition rates across the Zr isotopic chain. For the first time, the half-life of the 3^- state in ^{90}Zr, $T_{1/2} = 7.8(16)$ ps, was determined based on the plunger technique, and employing a ^{7}Li + ^{89}Y reaction, at sub-Coulomb barrier energy. The measured half-life of the 3^- state translates into the transition rate $B(E3; 3^- \rightarrow 0^+) = 16(3)$ W.u., which points to a significantly lower octupole strength than currently adopted in the database [1]. Now, this $B(E3)$ value is in line with the general monotonic increase observed along the Zr chain, from A = 90 to 96. In ^{91}Zr, the half-life of $T_{1/2}$ = 500(16) ps, for the $(11/2)^-$ state at 2170 keV, was also measured employing the fusion-evaporation reaction ^{13}C + ^{82}Se and fast-timing techniques. As a result, the $B(E3; (11/2)^- \rightarrow 5/2^+) = 20.5(7)$ W.u. transition rate was obtained, pointing to a sizable collectivity that may arise from the coupling of the valence $d_{5/2}$ neutron with the 3^- octupole phonon of the ^{90}Zr core.

Experimental values were compared with RPA and HCM model for the ^{90}Zr and ^{91}Zr isotopes, respectively. The theoretical calculations tend to overestimate the measured $B(E3)$ value for ^{90}Zr, and, in general, for all even-even Zr isotopes up to $A = 96$, although the general

TABLE I. Experimental and theoretical results for the 3^-, 4^-, and 5^- states in ^{90}Zr and $11/2^-$ states in ^{91}Zr. Excitation energies and B(Eλ; $J^\pi \rightarrow$ g.s.) are reported. The main components of the wave functions, calculated using RPA for ^{90}Zr and the HCM model for ^{91}Zr, are also presented (see text for details).

	$\mathbf{J}^\pi$	**Energy [MeV]**			**B(Eλ) [W.u]**			**Main components [%]**		
		Exp.	SLy5	SAMi-m60	Exp.	SLy5	SAMi-m60		SLy5	SAMi-m60
^{90}**Zr**	3^-	2.748	2.550	3.603	16(3)	24.6	29.7	$\pi p^{-1}_{3/2} g_{9/2}$	61.1	72.5
								$\pi f^{-1}_{5/2} g_{9/2}$	28.1	5.4
								$\pi p^{-1}_{1/2} g_{7/2}$	1.3	3.3
								$\nu p^{-1}_{1/2} g_{7/2}$	1.0	2.7
								$\nu g^{-1}_{9/2} h_{11/2}$	1.9	3.9
	4^-	2.739	1.907	3.576	-	0.8×10^{-1}	1.1×10^{-1}	$\pi p^{-1}_{1/2} g_{9/2}$	97.7	98.4
	5^-	2.319	1.550	3.089	8.74(33)[a]	8.5	9.8	$\pi p^{-1}_{1/2} g_{9/2}$	99.7	98.4
^{91}**Zr**	$11/2^-$	2.170	2.602	3.460	20.5(7)	19.6	14.4	$3^- \otimes \nu d_{5/2}$	78.2	47.8
								$0^+ \otimes \nu h_{11/2}$	11.6	14.9
	$11/2^-$	(2.320)	1.902	4.220	-	3.7×10^{-1}	0.7×10^{-1}	$4^- \otimes \nu d_{5/2}$	97.7	99.7
	$11/2^-$	(2.320)	1.502	3.818	-	7.6×10^{-1}	8.9	$5^- \otimes \nu d_{5/2}$	94.9	64.3
								$3^- \otimes \nu d_{5/2}$	2.7	31.2

[a] Adopted from Ref. [21].

trend is well reproduced. This suggests that the nature of the 3^- states along $Z = 40$ is dominated by collective octupole phonons to which neutron excitations significantly contribute. In ^{91}Zr, the HCM model describes the $(11/2)^-$ state located at 2170 keV in terms of a coupling of the unpaired neutron with the 3^- octupole excitation of the ^{90}Zr core, with a decrease of octupole strength. Experimentally, the measured $B(E3)$ value points to a collectivity stronger than in the ^{90}Zr core, which can not be explained in the weak-coupling limit. Further studies of $(11/2)^-$ excitations in the odd members of the Zr chain would be instrumental in delineating the microscopic nature of collective octupole-type excitations in these nuclei and, more generally, to the important topic of octupole correlations.

ACKNOWLEDGMENTS

This work was supported by the Polish National Science Centre, Poland, under research project No. 2020/39/D/ST2/03510, the Romanian MCID Nucleu program PN 23 21 01 02, and the Italian Istituto Nazionale di Fisica Nucleare.

[1] T. Kibedi and R. H. Spear, Atomic Data and Nuclear Data Tables **80**, 35 (2002).
[2] P. A. Butler and W. Nazarewicz, Rev. Mod. Phys. **68**, 349 (1996).
[3] A. Bohr and B. R. Mottelson, *Nuclear Structure Vol. 2* (World Scientific Publishing, Singapore, 1999).
[4] P. Van Isacker, The European Physical Journal Special Topics **229**, 2443 (2020).
[5] I. Hamamoto, Phys. Rep. **10**, 63 (1974).
[6] P. Bortignon, R. Broglia, D. Bes, R. Liotta, and V. Paar, Phys. Lett. B **64**, 24 (1976).
[7] P. Kleinheinz, Phys. Scr. **24**, 236 (1981).
[8] P. Kleinheinz, J. Styczen, M. Piiparinen, J. Blomqvist, and M. Kortelahti, Phys. Rev. Lett. **48**, 1457 (1982).
[9] M. Rejmund *et al.*, Eur. Phys. J. A **8**, 161 (2000).
[10] B. Fornal *et al.*, Phys. Rev. Lett. **87**, 212501 (2001).
[11] N. Pietralla *et al.*, Phys. Lett. B **681**, 134 (2009).
[12] S. Leoni, A. Bracco, G. Colò, and B. Fornal, Eur. Phys. J. A **55**, 247 (2019).
[13] C. Morse, A. O. Macchiavelli, H. L. Crawford, S. Zhu, C. Y. Wu, Y. Y. Wang, J. Meng, B. B. Back, B. Bucher, C. M. Campbell, M. P. Carpenter, J. Chen, R. M. Clark, M. Cromaz, P. Fallon, J. Henderson, R. V. F. Janssens, M. D. Jones, T. L. Khoo, F. G. Kondev, T. Lauritsen, I. Y. Lee, J. Li, D. Potterveld, C. Santamaria, G. Savard, D. Seweryniak, S. Stolze, and D. Weisshaar Phys. Rev. C **102**, 054328 (2020).
[14] V. Gillet, A. M. Green, and E. A. Sanderson, Nucl. Phys. **88**, 321 (1966).

[15] B. Bucher, S. Zhu, C. Y. Wu, R. V. F. Janssens, D. Cline, A. B. Hayes, M. Albers, A. D. Ayangeakaa, P. A. Butler, C. M. Campbell, M. P. Carpenter, C. J. Chiara, J. A. Clark, H. L. Crawford, M. Cromaz, H. M. David, C. Dickerson, E. T. Gregor, J. Harker, C. R. Hoffman, B. P. Kay, F. G. Kondev, A. Korichi, T. Lauritsen, A. O. Macchiavelli, R. C. Pardo, A. Richard, M. A. Riley, G. Savard, M. Scheck, D. Seweryniak, M. K. Smith, R. Vondrasek, and A. Wiens, Phys. Rev. Lett **116**, 112503 (2016).

[16] B. Bucher, S. Zhu, C. Y. Wu, R. V. F. Janssens, R. N. Bernard, L. M. Robledo, T. R. Rodríguez, D. Cline, A. B. Hayes, A. D. Ayangeakaa, M. Q. Buckner, C. M. Campbell, M. P. Carpenter, J. A. Clark, H. L. Crawford, H. M. David, C. Dickerson, J. Harker, C. R. Hoffman, B. P. Kay, F. G. Kondev, T. Lauritsen, A. O. Macchiavelli, R. C. Pardo, G. Savard, D. Seweryniak, and R. Vondrasek, Phys. Rev. Lett **118**, 152504 (2017).

[17] R. V. Jolos and P. von Brentano, Phys. Rev. C **92**, 044318 (2015).

[18] C. M. Baglin, Nuclear Data Sheets **113**, 2187 (2012).

[19] Ł. W. Iskra, R. Broda, R. V. F. Janssens, M. P. Carpenter, B. Fornal, T. Lauritsen, T. Otsuka, T. Togashi, Y. Tsunoda, W. B. Walters, and S. Zhu, Physics Letters B **788**, 396 (2019).

[20] P. E. Garrett, W. Younes, J. A. Becker, L. A. Bernstein, E. M. Baum, D. P. DiPrete, R. A. Gatenby, E. L. Johnson, C. A. McGrath, S. W. Yates, M. Devlin, N. Fotiades, R. O. Nelson, and B. A. Brown, Phys. Rev. C **68**, 024312 (2003).

[21] S. K. Basu and E. A. Mccutchan, Nucl. Data Sheets **165**, 1 (2020).

[22] R. P. Singhal, S. W. Brain, C. S. Curran, W. A. Gillespie, A. Johnston, E. W. Lees, and A. G. Slight, Journal of Physics G: Nuclear Physics **1**, 558 (1975).

[23] R. Liguori Neto, P. Roussel-Chomaz, L. Rochais, N. Alamanos, F. Auger, B. Fernandez, J. Gastebois, A. Gillibert, R. Lacey, A. Miczaika, D. Pierroutsakou, J. Barrette, S. K. Mark, R. Turcotte, Y. Blumenfeld, N. Frascaria, J. P. Garron, J. C. Roynette, J. A. Scarpaci, T. Suomijärvi, A. Van der Woude, and A. M. Van den Berg, Nuclear Physics A **560**, 733 (1993).

[24] W. S. Gray, R. A. Kenef ck, J. J. Kraushaar, and G. R. Satchler, Phys. Rev. **142**, 735 (1966).

[25] R. De Swiniarski, D.-L. Pham, G. Bagieu, and H. V. Geramb, Can. J. Phys. **57**, 540 (1979).

[26] J.R. Beene, D.J. Horen, and G.R. Satchler, Phys. Lett. B **344**, 67 (1995).

[27] G. A. Gill, R. D. Gill, and G. A. Jones, Nuclear Physics A **224**, 152 (1974).

[28] D. Bucurescu, I. Căta-Danil, G. Ciocan, C. Costache, D. Deleanu, R. Dima, D. Filipescu, N. Florea, D. G. Ghiţă, T. Glodariu, M. Ivaşcu, R. Lică, N. Mărginean, R. Mărginean, C. Mihai, A. Negret, C. R. Niţă, A. Olăcel, S. Pascu, T. Sava, L. Stroe, A. Şerban, R. Şuvăilă, S. Toma, N. V. Zamfir, G. Căta-Danil, I. Gheorghe, I. O. Mitu, G. Suliman, C. A. Ur, T. Braunroth, A. Dewald, C. Fransen, A. M. Bruce, Zs. Podolyák, P. H. Regan, O. J. Roberts, Nuclear Instruments and Methods in Physics Research Section A: Accelerators, Spectrometers, Detectors and Associated Equipment **837**, 1 (2016).

[29] T. Beck, C. Costache, R. Lică, N. Mărginean, C. Mihai, R. E. Mihai, O. Papst, S. Pascu, N. Pietralla, C. Sotty, L. Stan, A. E. Turturică, V. Werner, J. Wiederhold and W. Witt. Nuclear Instruments and Methods in Physics Research Section A: Accelerators, Spectrometers, Detectors and Associated Equipment **951**, 163090 (2020).

[30] D. Abriola and A. A. Sonzogni, Nucl. Data Sheets **107**, 2423 (2006).

[31] D. R. Tilley, H. R. Weller, C. M. Cheves, and R. M. Chasteler, **595**, 1 (1995).

[32] R. M. Pérez-Vidal, A. Gadea, C. Domingo-Pardo, A. Gargano, J. J. Valiente-Dobón, E. Clément, A. Lemasson, L. Coraggio, M. Siciliano, S. Szilner, M. Bast, T. Braunroth, J. Collado, A. Corina, A. Dewald, M. Doncel, J. Dudouet, G. de France, C. Fransen, V. González, T. Hüyük, B. Jacquot, P. R. John, A. Jungclaus, Y. H. Kim, A. Korichi, M. Labiche, S. Lenzi, H. Li, J. Ljungvall, A. López-Martens, D. Mengoni, C. Michelagnoli, C. Müller-Gatermann, D. R. Napoli, A. Navin, B. Quintana, D. Ramos, M. Rejmund, E. Sanchis, J. Simpson, O. Stezowski, D. Wilmsen, M. Zielińska, A. J. Boston, D. Barrientos, P. Bednarczyk, G. Benzoni, B. Birkenbach, H. C. Boston, A. Bracco, B. Cederwall, D. M. Cullen, F. Didierjean, J. Eberth, A. Gottardo, J. Goupil, L. J. Harkness-Brennan, H. Hess, D. S. Judson, A. Kaşkaş, W. Korten, S. Leoni, R. Menegazzo, B. Million, J. Nyberg, Z. Podolyak, A. Pullia, D. Ralet, F. Recchia, P. Reiter, K. Rezynkina, M. D. Salsac, M. Şenyiğit, D. Sohler, C. Theisen, and D. Verney, Phys. Rev. Lett. **129**, 112501 (2022).

[33] N. Mărginean, D. L. Balabanski, D. Bucurescu, S. Lalkovski, L. Atanasova, G. Căta-Danil, I. Căta-Danil, J. M. Daugas, D. Deleanu, P. Detistov, G. Deyanova, D. Filipescu, G. Georgiev, D. Ghiţă, K. A. Gladnishki, R. Lozeva, T. Glodariu, M. Ivaşcu, S. Kisyov, C. Mihai, R. Mărginean, A. Negret, S. Pascu, D. Radulov, T. Sava, L. Stroe, G. Suliman and N. V. Zamfir, The European Physical Journal A **46**, 329–336 (2010).

[34] T. Kibédi, T.W. Burrows, M.B. Trzhaskovskaya, P.M. Davidson, C.W. Nestor, Jr., Nuclear Instruments and Methods in Physics Research Section A: Accelerators, Spectrometers, Detectors and Associated Equipment A **589**, 202 (2008).

[35] G. Colò, L. Cao, N. Van Giai, and L. Capelli, Computer Physics Communications **184**, 142 (2013).

[36] E. Chabanat, P. Bonche, P. Haensel, J. Meyer, and R. Schaeffer, Nuclear Physics A **635**, 231 (1998).

[37] X. Roca-Maza, M. Brenna, B. K. Agrawal, P. F. Bortignon, G. Colò, L.-G. Cao, N. Paar, and D. Vretenar, Phys. Rev. C **87**, 034301 (2013).

[38] G. Colò, P. F. Bortignon, and G. Bocchi, Phys. Rev. C **95**, 034303 (2017).

[39] G. Bocchi, S. Leoni, B. Fornal, G. Colò, P.F. Bortignon, S. Bottoni, A. Bracco, C. Michelagnoli, D. Bazzacco, A. Blanc, G. de France, M. Jentschel, U. Köster, P. Mutti, J.-M. Régis, G. Simpson, T. Soldner, C.A. Ur, W. Urban, L.M. Fraile, R. Lozeva, B. Belvito, G. Benzoni, A. Bruce, R. Carroll, N. Cieplicka-Oryńczak, F.C.L. Crespi, F. Didierjean, J. Jolie, W. Korten, T. Kröll, S. Lalkovski, H. Mach, N. Mărginean, B. Melon, D. Mengoni, B. Million, A. Nannini, D. Napoli, B. Olaizola, V. Paziy, Zs. Podolyák, P.H. Regan, N. Saed-Samii, B. Szpak and V. Vedia, Physics Letters B **760**, 273 (2016).

[40] S. Bottoni, N. Cieplicka-Oryńczak, S. Leoni, B. Fornal, G. Colò, P. F. Bortignon, G. Bocchi, D. Bazzacco, G. Benzoni, A. Blanc, A. Bracco, S. Ceruti, F. C. L. Crespi, G. de France, E. R. Gamba, Ł. W. Iskra, M. Jentschel,

U. Köster, C. Michelagnoli, B. Million, D. Mengoni, P. Mutti, Y. Niu, C. Porzio, G. Simpson, T. Soldner, B. Szpak, A. Türler, C. A. Ur, and W. Urban, Phys. Rev. C **103**, 014320 (2021).

[41] G. Colò, H. Sagawa, and P. F. Bortignon, Phys. Rev. C **82**, 064307 (2010).

[42] D. K. Sharp, B. P. Kay, J. S. Thomas, S. J. Freeman, J. P. Schiffer, B. B. Back, S. Bedoor, T. Bloxham, J. A. Clark, C. M. Deibel, C. R. Hoffman, A. M. Howard, J. C. Lighthall, S. T. Marley, A. J. Mitchell, T. Otsuka, P. D. Parker, K. E. Rehm, D. V. Shetty, and A. H. Wuosmaa, Phys. Rev. C **87**, 014312 (2013).